NUMERICAL STUDY OF AERODYNAMIC HIGH SPEED PROPELLER ENGINE INTEGRATION ON TRANSPORT AIRCRAFT

P. COLIN
V. MOREUX
A. BARILLIER
Aerodynamic Design Department
Aerospatiale - Aircraft Business
316, route de Bayonne 31060 TOULOUSE CEDEX03
FRANCE

Abstract

Within the framework of preliminary studies relative to the FLA project, Aerospatiale has designed a wind-tunnel model. The purpose is to get an initial experimental estimation of engine installation effects on such an aircraft, including propeller / airframe interference.
Numerical tools have been widely used to define the external shapes of the nacelles to be mounted on this model. Due to the high cruise Mach number of the FLA, Euler solvers have been used complementarily to our basic panel method, viscous effects being assessed through boundary layer calculations.
All these solvers include a propeller modelling capability, based on the actuator disk technique. Isolated propeller calculations using a lifting line based code were performed to feed these actuator disks.
This last code has also been used, together with Euler simulations in a rotating frame, to analyse different preliminary propellers, in order to check their ability to provide the required level of thrust on the model.
In the first part of the paper, the different codes involved, and the way they are used within the design process are introduced with some validations on ATR configurations. Examples of their use for the model design are then presented.

1. Introduction

Engine airframe integration is part of Aerospatiale's major responsibilities within the worksharing relevant to both AIRBUS and ATR aircraft families. Preliminary studies relative to the Future Large Aircraft (FLA) have led us to enhance our numerical toolkit in order to better take the aerodynamic propeller influence into account, within the engine integration design process.

The FLA is a high wing propeller-driven military cargo aircraft, jointly designed by the major European airframe manufacturers, for ambitious high speed and low speed requirements. FLA specifications impose a 0.68 / 0.72 range cruise Mach number (between 0.45 and 0.5 for the ATR family). At such Mach numbers, compressibility effects, even increased by propeller blowing, can become large. Airframe and propellers have to be designed accordingly. Appropriate validated solvers for propeller or aircraft aerodynamic analysis then become precious tools for design engineers who are faced with this new challenge.

Engine installation is designed so as to minimize the aircraft performance loss it induces, while taking various feasibility constraints into account. Parts of the aircraft situated in the wakes of the propellers experience a complex time-dependent flow, which modifies their aerodynamic responses. These propeller effects (increase in total pressure and axial velocity, creation of a rotational velocity...) are superimposed on the classical installation effects (local lift decrease, flow acceleration on the wing lower surface...). One way to optimize the aerodynamic engine integration is often to minimise these effects, and check that they do not induce any undesirable phenomena like strong shocks or separations.

This paper aims at showing what kind of numerical tools are used at Aerospatiale for such design work, and how they are used to select the most promising shapes before wind-tunnel validations.

2. Numerical toolkit for propeller simulation

2.1. What tools for what needs?

Numerical simulation of propeller / aircraft interference can be achieved at different levels of complexity. The available power on the most recent parallel super computers makes unsteady Euler or even averaged Navier-Stokes calculations possible, mixing fixed parts (aircraft) and rotating parts (propeller). Nevertheless a simplified approach, considering time-averaged modelling of the propeller wake can provide the design engineer with interesting information at a much lower computational cost. The latter approach is the one used at present at Aerospatiale, the former being under study within the framework of a cooperation between Onera and Aerospatiale.

At the early stages of the design process of a new engine installation, the design engineer usually faces a large number of possible configurations. He has to investigate various elementary effects (engine position..) and design strategies (use of a pylon or not, if not, position of the wing / nacelle intersection with respect to the wing leading edge...). For the aerodynamic analysis of all these configurations, he needs quick responses and therefore an easy-to-use solver. Furthermore, he does not always need a very complex physical model, since such effects are

generally large in magnitude and since he is often only looking for trends.
When design becomes finer, the need for better precision arises, and more complex physical models have to be used.

Aerospatiale has three operational solvers for propeller / airframe interaction calculations, all based on the principle of an actuator disk for propeller modelling.
The simplest one is the inhouse FP3D panel method (see § 2.3.1.). The second one solves the Euler equations over cartesian grids ; it is the MGAERO solver distributed by AMI (see § 2.3.2.). The last one is the multiblock Euler / Navier-Stokes CANARI solver developed at Onera (see § 2.2.2. and § 2.3.3.). CANARI is not yet commonly used for viscid calculations within the design process. Viscous effects are assessed through boundary layer calculations with the 3C3D program, developed at Cert/Onera (see § 2.3.4.), which can be operated at a very low cost after each inviscid calculation by FP3D or CANARI.

All the grids required by these codes, grids of the aircraft skin for FP3D and the MGAERO preprocessor (the cartesian volumic grid is created within MGAERO), and volumic grids for CANARI are constructed with the ICEM-CFD package developed by CONTROL DATA SYSTEMS in cooperation with Aerospatiale [1]. ICEM-CFD operates in interactive mode on a workstation which allows a high flexibility when constructing grids around complex configurations. For the most frequently used topologies, an automatic procedure is used through the ICEM-CFD COMAK tool : a command file is created the first time a geometry is meshed using the topology, which can be replayed for the following geometries. In replay mode, the user manual intervention is limited to some possible tuning of grid clustering to improve its quality.

The time required for one fine mesh analysis cycle on a complex configuration can approximately be broken down for each solver as shown in table 1. Computational times are given on one processor of Aerospatiale's CRAY J916, except for MGAERO which runs on SGI workstations (F refers to first mesh, and R to replay mode).

	mesh generation	calculation
FP3D	2 days (F) 0.5 day (R)	1 hour
MGAERO	2 days (F)	1 night
CANARI	10 days (F) 1 to 2 days (R)	1 to 2 nights

Table 1

FP3D is particularly suitable for preliminary design calculations. Its very short cycle allows several geometries to be analysed during the day and it is largely operated by design engineers.
An initial approach to compressibility can be obtained with MGAERO, which can provide one result every day. It is therefore used as an intermediate tool in the design process. It can also supply a quick answer to a given problem involving compressibility effects.

The best precision is obtained with CANARI, but its larger cycle limits its use to the last steps of the design process.

The different actuator disks involved in the FP3D, MGAERO and CANARI codes require some specific data, ranging from load distributions on the blade for FP3D, to radial distributions of mean jumps in total pressure, total temperature and velocity for both Euler solvers. These data can be obtained either directly from the propeller manufacturer through dedicated tools called propeller decks (full-scale propeller characteristics database, consisting of a mixture of experimental results and numerical calculations), or by using isolated propeller analysis codes. Two codes are available at present at Aerospatiale for this purpose : the inhouse HLPQ code, based on the lifting line theory (see § 2.2.1.), and the CANARI code, used in a rotating frame (see § 2.2.2.).

These programs can also be used for isolated propeller performance assessment, which corresponds to another need of design engineers. In this way they can check that a given propeller is able to achieve the required level of efficiency in various flight conditions.

The way all the codes mentioned above are linked together is summarized on figure 1. The following paragraphs provide more details on these programs and give some elements of validation, mainly on ATR configurations.

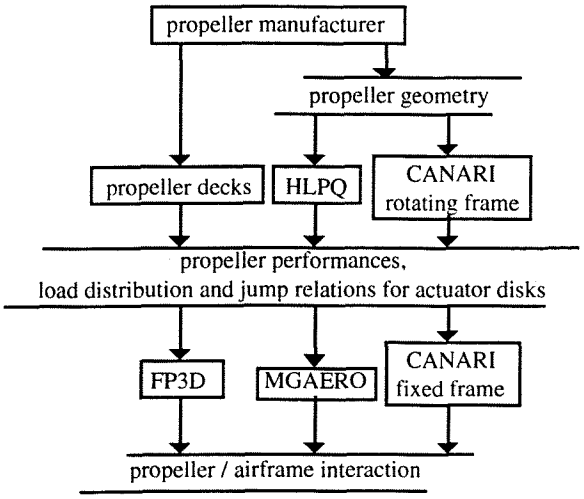

Figure 1
Toolkit for propeller simulations

2.2. Isolated propeller simulations

2.2.1. HLPQ lifting line program

The first step before analysing the complex interaction between propellers and geometries consists in estimating the isolated propeller performance (thrust, torque, efficiency) together with the aerodynamic characteristics of the slipstream that it generates.

Until recently, Aerospatiale entirely relied on the propeller manufacturer to get this information. Flight testing or wind-tunnel measurements were the only way to check whether the levels of efficiency announced were correct or not.

In order to improve its capability of calculating these propeller performance and characteristics, Aerospatiale has recently developed the HLPQ code based on the lifting line theory [2,3]. The blade is represented by the swept mid-chord line bearing a set of helicoidal horseshoe vortices of varying pitches, whose intensities equal the local circulations Γ. The circulations are computed through an iterative procedure : at every control point the induced velocities can be calculated from a given Γ distribution by the Biot and Savart formulae. Local pitches of the horseshoe vortices and local angle-of-attack of every airfoil along the radius can be then derived. An updated Γ distribution is then obtained using the well-known Prandtl assumption relating the local circulation to the effective angles-of-attack "seen" by the airfoils. The convergence criterion is based on the variation in pitch of every horseshoe vortex.

In order to calculate the 2D-aerodynamic characteristics of every profile (needed by the Prandtl assumption), we make use of the 2D interactive Euler and Boundary Layer code ISES [4]. This approach allows us to insert both viscous and compressibility effects in our calculations. To account for the 3D aspect of the blade (sweep and dihedral), we apply the swept-wing theory to the coefficients determined by ISES before using them in HLPQ.

Many calculations have been performed on different propellers (conventional or of propfan type) which have proved the method to be accurate and robust. Table 2 summarizes the performance calculated for two ATR-type propellers, P1 and P2, for two operational points, "near climb" (Mach=0.18) and "near cruise" (Mach=0.51). The difference between these two propellers lies in their sweep angle and number of blades. Results are compared to experimental data and show good agreement (within two percent).

	P1	P2
η(calc.) / η(exp.) (Near Climb)	0.986	0.980
η(calc.) / η(exp.) (Near Cruise)	0.983	0.980

Table 2

Concerning the local characteristics of the flowfield around the blade or in the slipstream, very few experimental data were available. For both propellers we could only compare the lift distribution along the blade with some calculations performed by the manufacturer himself. Figures 2 and 3 show good agreement except perhaps at the root of the P1-propeller where our discretization is too coarse.

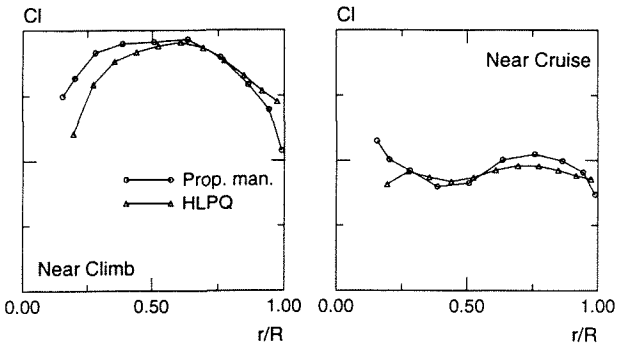

Figure 2
P1-Propeller lift distributions

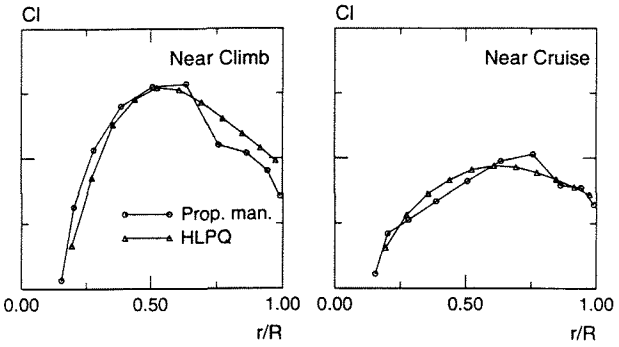

Figure 3
P2-propeller lift distributions

The only experimental data at our disposal consisted of LDV (Laser Doppler Velocimetry) measurements around several profiles of the P2-propeller run in an isolated configuration at Mach 0.494. The experimental circulation distribution was computed by integrating the velocity along rectangular paths enclosing those profiles. Beam reflections at the hub led to inaccurate results on the first half of the blade. As shown on figure 4, experimental data are scattered. This is due to the choice of the blade around which measurements are performed but also to the size of the integration path chosen. The circulations calculated by HLPQ agree quite well with experience especially on the most outboard part of the blade.

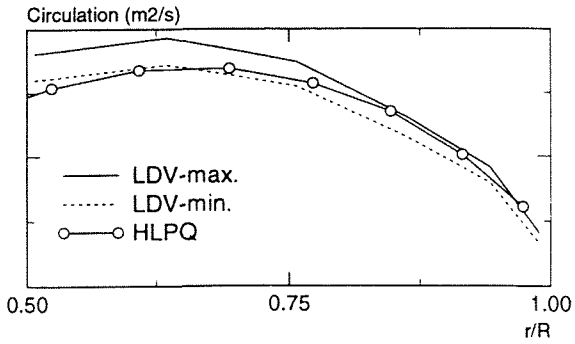

Figure 4
P2-propeller circulation distribution

Further to propeller performance assessment, results from HLPQ can be post-processed in order to feed the actuator disk models implemented in FP3D, MGAERO and CANARI as mentioned earlier in this article.
The axial velocities are averaged at every radius using the Siestrunck approach [3]. The averaged tangential velocities can then be calculated using the blade element theory [5]. From these averaged velocities, we can calculate the angular deviations experienced by the flow at the propeller plane (contraction and swirl).
The total pressure and total temperature jumps through the propeller plane are estimated from the averaged induced velocities. The former uses a Froude approach with a compressibility correction, and the latter uses the Euler equilibrium which constitutes a classic result of the turbomachinery theory.

2.2.2. CANARI multi-block Euler solver

Aerospatiale has been using the CANARI Euler / Navier-Stokes solver since the early nineties, at first for calculations of flow fields around turbofan engine installation configurations [6,7,8], and more recently for both isolated propeller simulations and assessment of propeller slipstream / airframe interactions.

This solver, called SESAME before its extension to viscous flow simulations, has been developed at Onera [9,10]. CANARI solves the 3D time-dependent Reynolds averaged Navier-Stokes equations, in a cartesian coordinate system rotating with angular velocity Ω about the x axis. It is based on a multiblock structured approach.
The numerical resolution is inspired by the scheme proposed by Jameson [11]. Spatial discretization is achieved through a finite volume cell-centered formulation, and a centered scheme is used for flux calculations. An artificial viscosity is added to stabilize the scheme and to capture flow discontinuities. A 4-step Runge-Kutta scheme associated with a scalar implicit phase is used for time integration. Local time stepping and full multigrid allow convergence to steady state to be accelerated.
Boundary conditions are treated according to the characteristic relations theory. A characteristic relation is used when the corresponding "information" propagates from inside to outside of the computational domain. Otherwise a complementary relation is used.

A COMAK automatic grid generation procedure has been developed for CANARI isolated propeller simulations. The advantage of this automation is twofold : it of course allows the meshing of a new propeller geometry to be simplified, but above all, it makes quick change in the blade pitch angle possible. A large number of thrust coefficients can then be investigated.
A two-block topology is used. A C-H block is placed around the blade, and an H-H block upstream of the blade. These two blocks extend in azimuth up to the periodicity boundaries which are approximately situated on two consecutive blade to blade mean surfaces (figure 5).
CANARI Euler calculations in a rotating frame are complementary to calculations performed with the HLPQ lifting line program. They do not take viscous effects into account (thus inducing an overestimated efficiency), but nevertheless they provide real 3-dimensional simulations which can be useful to understand certain flow features (for instance in the blade tip region).

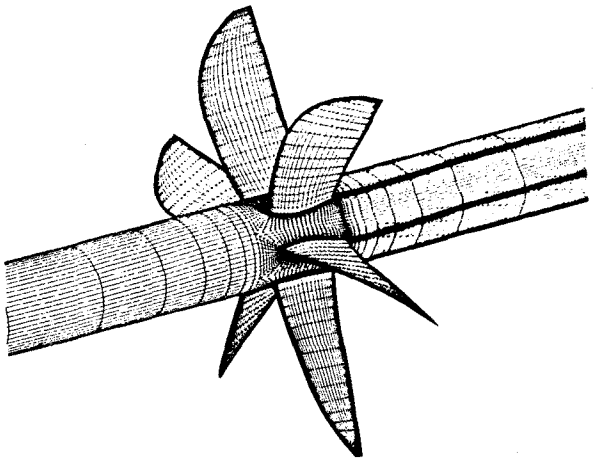

Figure 5
Grid around a complete FLA-type propeller

Furthermore CANARI can give a better evaluation of transonic blade-to-blade interaction. For instance we can check that there is no flow blockage nearby the spinner (figure 6, where the solid line represents the iso Mach=1 line).

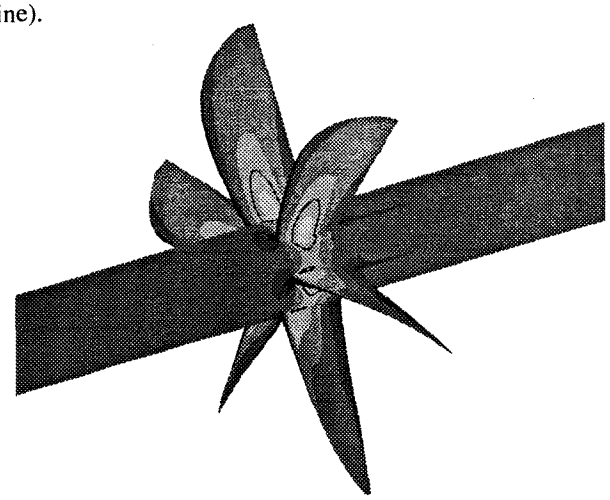

Figure 6
Mach contours on a complete FLA-type propeller in cruise conditions

2.3. Propeller / Airframe interaction

2.3.1. FP3D Panel method

Aerospatiale has developed the inhouse FP3D [12] panel method since 1985, for subcritical flow calculations about the most general configurations.

It is based on a velocity formulation with Neuman boundary conditions. Compressibility is taken into account through a method proposed by B.Hunt [13]. The

aircraft surface is discretized into quadrangular or triangular panels, bearing a constant source singularity. For lifting elements such as wing or pylon, a chordwise linear and spanwise piecewise constant distribution of horseshoe vortices is added on a mean "squeleton" surface situated between the pressure and suction sides. The trailing vortices of this distribution form the wake of the lifting element. Their positions can be assumed to be known, or relaxed through an iterative procedure to cancel the normal velocity on the wake.
Another interesting feature of the FP3D code is its ability to simulate non uniform initial flows. In such a case, a distribution of perturbation velocities is added, which modifies the writing of the boundary conditions on the panel control points. Jumps on total pressure can be specified as well for the calculation of pressure coefficients from velocities. Perturbation velocities and total pressure jumps are computed by different pre-processors, depending on the kind of perturbations that are to be modelled.

The pre-processor used for propeller wake modelling is based on the method proposed by C.Kirrmann et al (5). The time-averaged propeller slipstream is materialized by a distribution of vortex singularities placed on rings and tubes, centered on its mean axis (figure 7). One takes the wake contraction into account empirically, using the Froude theory.

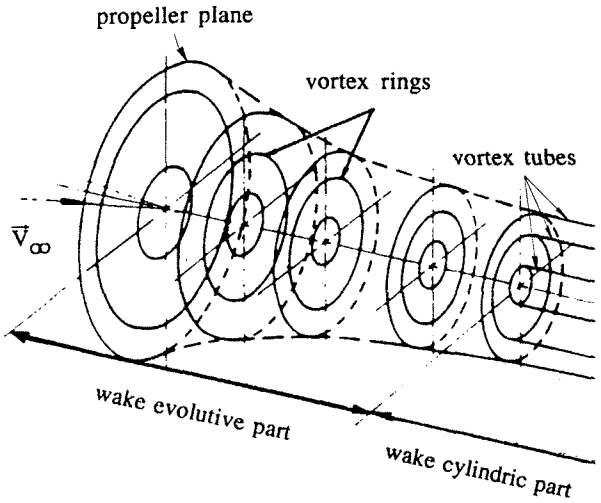

Figure 7
Vortex distribution used in the FP3D pre-processor for propeller wake modelling

The intensities of the vortices situated at each radial station are computed from the load distribution on the blade, which is an input of the program, and can be obtained from HLPQ calculations.
Resulting axial perturbation velocities are directly computed by summing the contributions of the different vortices. Tangential velocities are then assessed in the propeller plane according to the blade element theory. The kinetic momentum conservation allows them to be computed downstream of this plane.

Total pressure jumps are finally calculated from these velocities, in the same way as presented in §.2.2.1, for HLPQ post-processing.

2.3.2. MGAERO Euler solver in cartesian grids

The MGAERO (MultiGrid AEROdynamics) code (14,15) solves the three-dimensional Euler equations about arbitrary configurations.

The geometry is defined by surface paneling of its different components (fuselage, wing, pylon, ...). The solver automatically takes the intersection between the components into account, allowing them to interpenetrate each other. Each component must be defined by a set of parallel sections composed of an array of points.

The main originality of MGAERO is the use of cartesian grids : unlike most solvers, the grids do not need to be body-fitted. This particularity reduces the grid production time from weeks to one or two days. The difficulty is thus transferred to the solver that has to correctly treat the slip condition on solid surfaces.

Symmetrical difference schemes are used for second-order accurate approximation of the spatial discretization. Dissipative terms are introduced (11) to stabilize the scheme and to avoid non-physical solutions. A 4-step Runge-Kutta time marching scheme is used, as well as residual smoothing to accelerate convergence. The solver allows for multigrid with local refinements : the grids are selectively refined by the user in order to improve the accuracy in regions of interest.

A simple propeller modelling, via an actuator disk representation, is implemented in MGAERO. Radius dependent outflow swirl angle and jumps (with respect to the free stream values) in normal outflow velocity, total pressure and total temperature are specified in the input files.

2.3.3. CANARI multi-block Euler solver

The CANARI solver (see § 2.2.2.) is used for propeller / airframe interaction calculations as well. In this case, the angular velocity Ω is evidently set to zero.

The propeller is modelled by a discontinuity surface on which specific boundary conditions are applied, one at the propeller front face, and one at the rear face. At the front face (subsonic outflow), the complementary relation used is a cell-to-cell continuity of the mass flow with respect to the rear face. At the rear face (subsonic inflow), jumps in total pressure, total temperature and velocity direction with respect to the front face constitute the four needed complementary relations. These jumps are a function of both radial position on the propeller, and local Mach number M_f at this location on the front face. They are given in the form of tables, jump = $f(r/R,M_f)$, by the user. Compared to those of FP3D or MGAERO, the CANARI actuator disk is richer since an influence of airframe on the

propeller is taken into account through the local front Mach number M_f.

2.3.4. 3C3D boundary layer code

The three-dimensional boundary layer code 3C3D (16,17) was developed at Cert/Onera. It was designed to handle complex flow configurations on realistic geometries.

The two main numerical particularities of the method are :
- integration of the equations along local streamlines, thus avoiding the difficulties related to direction changes of the cross-flow in the calculation domain,
- discretization of the equations at a given station in the plane tangent to the surface at this point. This technique relaxes the mesh regularity hypothesis associated with methods using generalized coordinates.

A marching technique is utilized in space to integrate the equations. This imposes that one family of mesh lines is roughly aligned with the flow direction. To cope with the geometric complexity of industrial applications, the solver allows for multiblock meshes with non-coincident nodes at the interfaces. However, these blocks must follow each other in the flow direction.

2.3.5. Validation on an engined nacelle

Wind-tunnel testing was conducted in 1994 for both P1- and P2-propellers (already mentioned in §2-2-1) installed on a 1/4-scaled ATR-type nacelle. A wide range of Mach numbers, advance ratios, thrust coefficients and pitch angles was covered, the results mainly consisting of pressure measurements on the skin. As shown on figure 8, there are 8 rows (A to H) of about 12 pressure taps each, regularly located at different azimuths around the nacelle.
For one specific run of the P1-propeller on this nacelle, LDV measurements were performed in order to get the three components of the velocity in three planes parallel to the propeller plane of rotation, one located upstream and two downstream, and for ten different azimuths (AZ1 to AZ10).

All the codes described above (FP3D, MGAERO and CANARI) were run on this specific configuration. Four run points were selected among the experimental data, three dedicated to Cp comparisons (one with no propeller installed called "tare" and one for each propeller) and one dedicated to LDV measurements. In the former case, all the three codes were used whereas in the latter only CANARI was run.

-Cp comparisons

We focused our analysis on the left-hand side of the nacelle where the blade goes down (rows C and D). Indeed, the blowing effect is maximum in this area where the propeller slipstream impacts the geometry. Figures 9 to 12 show how this blowing effect is seen on both rows C and D, either by experience or by the different codes used (FP3D, MGAERO, CANARI).

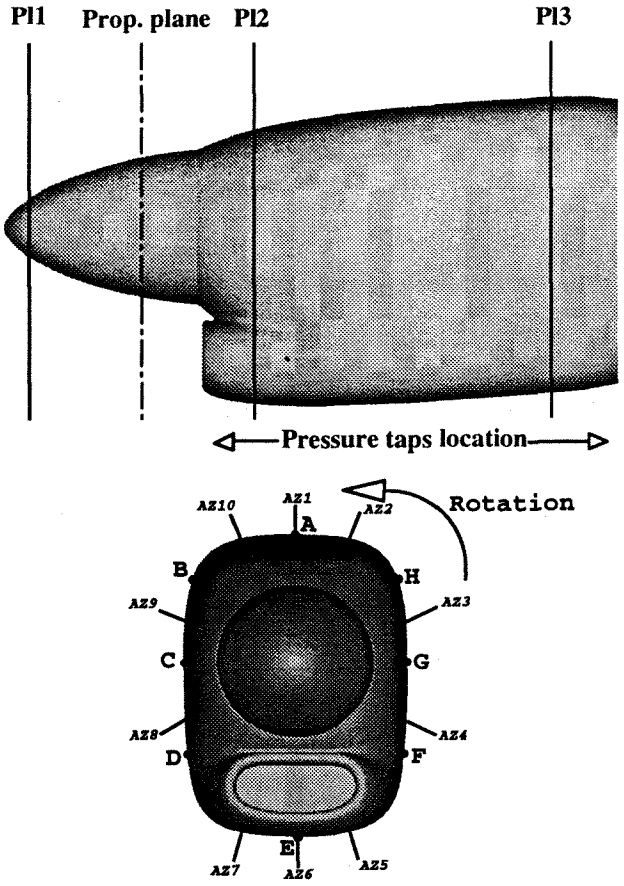

Figure 8
Nacelle geometry - location of pressure taps (rows A to H) - LDV measurements in planes PL1 to PL3 for azimuthal cuts AZ1 to AZ10

From those curves the following remarks can be drawn :
- as expected, the blowing effect is more visible on row D than on row C and this phenomenon is well captured by the different tools,
- there is hardly a difference between the effects induced by the P1-propeller and those induced by the P2-propeller. This is also reproduced by the calculations. It can also be noticed that the small differences in the computations between the two propellers are consistent throughout the diverse codes used.

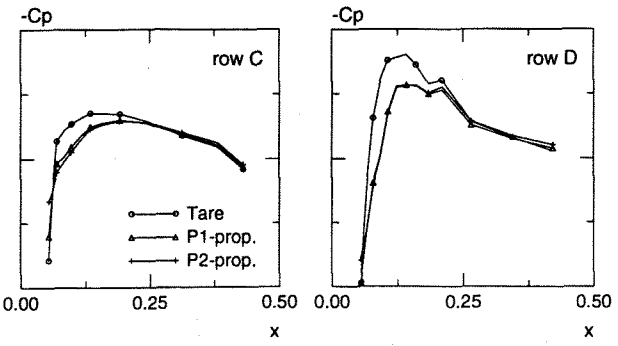

Figure 9
Blowing effect measured in wind-tunnel

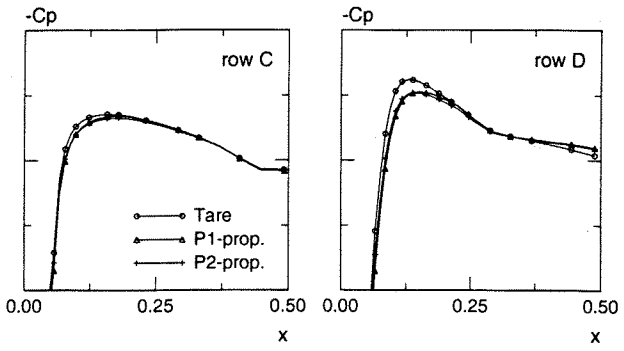

Figure 10
Blowing effect calculated by FP3D

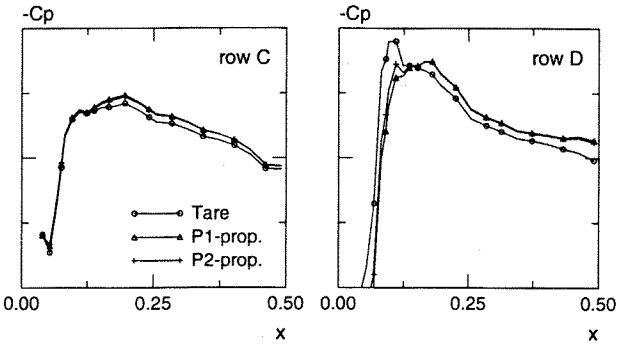

Figure 11
Blowing effect calculated by MGAERO

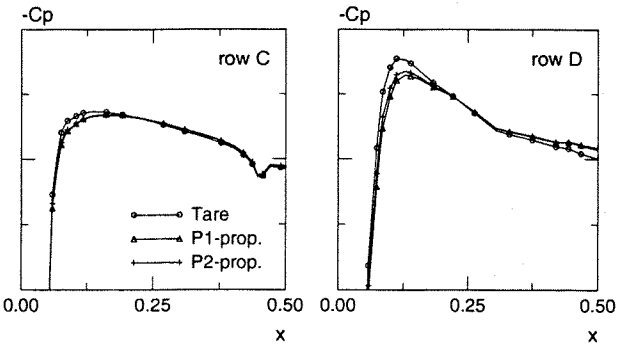

Figure 12
Blowing effect calculated by CANARI

- MGAERO seems to have a different behavior since the blowing effect is still visible far downstream of the propeller plane. The chaotic appearance of the curves that one can note, is provoked by the use of quite a coarse grid for MGAERO calculations.

LDV comparisons

Let us now look at the results obtained in the plane located just downstream of the propeller for the two azimuth cuts corresponding approximately to the rows where the pressure coefficients have been analyzed (that is AZ7 and AZ8). Figure 13 compares, for the three components, the velocity measured in the wind-tunnel with the P1-propeller rotating, and the velocities calculated by CANARI with and without propeller.

The following conclusions, valid for both azimuth cuts, can be drawn :

- the curve shape of the axial velocity is well reproduced by CANARI,
- there is remarkably good agreement on the tangential velocities between experience and the calculations. This is all the more notable as the shape of the curves are radically different. Since one of the major propeller installation effects lies in the modification of the angles-of-attack experienced by the wing profiles located behind the propeller, the good agreement noted hereabove makes us expect quite good results when calculating propeller / wing interaction,

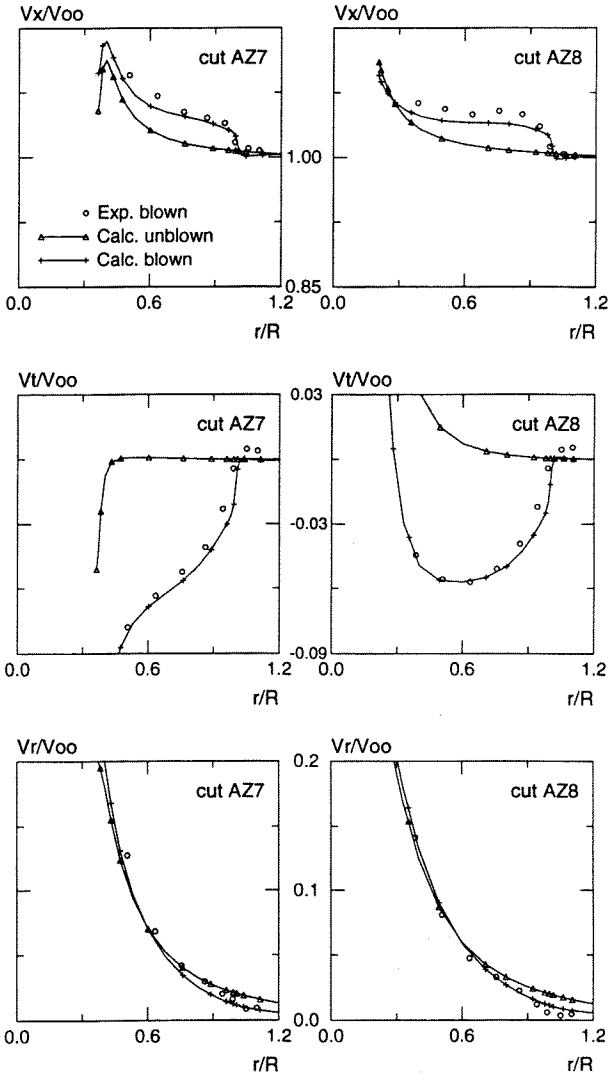

Figure 13
Velocity around the nacelle - Cuts AZ7 and AZ8
CANARI vs Experience

- the effect on radial velocity is very small since this component is more due to the flowfield going around the nacelle than to a propeller induced effect. One can note

though that the trend, however small it is, is well respected.

3. Application to design of a Future Large Aircraft (FLA) model

3.1. Introduction

A 1/9.5 half-model of a preliminary FLA geometry has been designed for engine installation testing at both high and low speed (leading edge and trailing edge can be replaced with high lift devices), with particular interest for propeller / airframe interaction assessment.

It comprises a left wing, a fuselage and both the inboard and outboard nacelles. Different nacelle external shapes can be investigated by replacing some parts of their cowls. Both nacelles can be equipped with engine simulators for propeller-on simulations, propeller rotating clockwise. This sense of rotation is more severe for the wing lower surface on which, inboard of the two nacelles, high suction peaks can be expected at low C_L.
In order to reduce the costs, one existing propeller (called hereafter FLAPP1) has been first considered as a good candidate to be mounted on the model. Different studies (including numerical studies, see § 3.2) made us ask the propeller manufacturer for a new design (propeller FLAPP5) so as to achieve a sufficient level of performance.

Model instrumentation comprises :
- a 6-component wall balance for global forces and moments measurements,
- one torquemeter in each nacelle,
- a 6-component propeller balance for installed propeller thrust calibration,
- measurements of blade pitch angle and propeller rotational speed,
- a large number of pressure taps, located on the wing, fuselage and both nacelles.

The first tests with this model are planned in September 1996 at Onera S1 Modane wind-tunnel. These high speed tests will provide a preliminary experimental assessment of installation effects, including propeller blowing, which will be useful to guide future work for design of the FLA engine installation.

The following paragraphs show some examples of applications of numerical methods, which have been performed for the model design. Calculations were made on the right wing and half fuselage, with anticlockwise rotating propellers, which is equivalent to the model configuration.

3.2. FLA model propellers analyses with HLPQ

Thanks to its ability to analyse the aerodynamics of propellers, Aerospatiale decided to take an active part in the preliminary studies of propellers specifically dedicated to the model, the purpose being to check that they were well suited to their foreseeable use.

The strategy of the use of HLPQ for such an objective is now described and can be split into two parts :

Analysis on design points

Design points correspond to specific operating conditions (take-off, cruise and so on) for which a certain level of performance is required for the propeller. They are used by the manufacturer as baseline for designing it.

To Aerospatiale, the starting point is the supply, by the manufacturer, of a propeller geometry. This usually goes together with the supply of a specific deck that gives the efficiency of the full-scale propeller for a wide range of operating conditions.

The first step is then the geometric analysis of the blade. It already gives (by comparison with previously studied propellers) a good idea of the aerodynamic behavior to be expected from the new one. In the second phase, HLPQ calculations are performed for the design points. Efficiencies thus obtained can then be compared with the ones announced by the manufacturer. Good agreement is indeed observed most of the time. Since the lift coefficient distribution as a function of the radius is also obtained, ISES can be run for several stations along the blade to get local aerodynamic characteristics.

Analysis of the propeller model behavior

Beyond the analysis of the full-scale propeller on very specific points the objective is to evaluate the behavior of its scaled model for the wind-tunnel conditions to be investigated. Furthermore, it is also necessary to determine the range of those conditions for which the flow is not likely to experience strong shocks or massive separations because of the vibrations it could involve.
These analyses are performed through the joint use of the specific deck (for it is an easy-to-use code that allows the propeller performance maps to be drawn quickly) and of HLPQ. The procedure is as follows :
- for the experimental conditions, the full-scale performance maps are drawn with the specific deck,
- associated HLPQ analyses are performed in order to calibrate it with respect to the deck,
- to evaluate the scale effect, these analyses are also performed on the scaled propeller. What is usually noted is a slight decrease in efficiency (about a 2%-shortfall to be applied to deck values). Moreover it is also possible to determine, for a given Mach number and angular velocity, the maximum thrust coefficient attainable before ISES detects a separation. It will then be considered that the propeller shouldn't be operated beyond this thrust.

What we finally get are :
- performance maps corrected to take scale effect into account,
- a range of "reachable" thrusts that can be compared to what was initially planned for the experimental campaign. If it is too restrictive, the first solution is to ask the manufacturer for a better propeller, the second (in case of

lack of time) to be more cautious and less ambitious on the campaign programme.

Application to FLA model propellers

- Analysis of FLAPP1 for FLA cruise design point :

As mentioned in § 3.1., Aerospatiale had first intended to use the existing FLAPP1 propeller, whose design points corresponded to lower Mach numbers than those to be tested in the wind-tunnel. Its analysis at FLA cruise design point Mach=0.68 effectively led to low full-scale and model efficiencies. ISES analysis indicated massive shock-induced separations in both cases. This behavior was still present for thrust coefficients as low as 0.1.

For better understanding of the aerodynamics of this propeller, it was decided to perform the same analysis for Mach=0.65 so as to check whether these phenomena were still occurring. Figure 14 summarizes this new analysis. A good agreement can be noted between the deck and HLPQ (full scale) and the Reynolds effect can be seen. The curves also show the maximum thrust coefficients (still too small) attainable before ISES detects a separation.

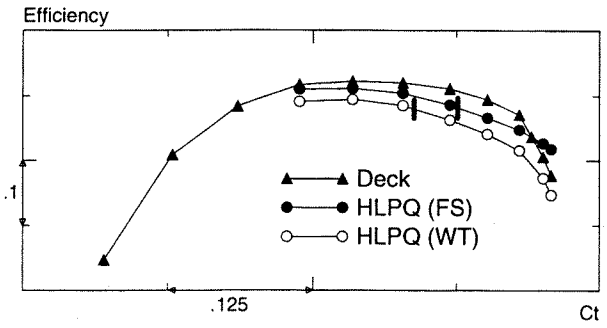

Figure 14
FLAPP1 analysis by HLPQ

The conclusion drawn from both analyses was that this propeller would not meet the requirements aimed at for the wind-tunnel campaign and that another one should be designed. After several iterations between Aerospatiale and the manufacturer, a sufficiently satisfactory propeller (FLAPP5) was finally designed and manufactured.

- Analysis of FLAPP5 for FLA max cruise design point

At Mach=0.72, there is very good agreement between the deck and HLPQ (see table 3 where FS refers to the full scale and WT to the scaled model). ISES detects no separation for thrust coefficients as high as 0.5 which is far beyond our expectations. The Reynolds effect leads to a 2.6% loss in efficiency.
This propeller seems to be well suited even for such a high Mach number and would cause no problem at all at Mach=0.68. In that case, our analysis shows that full-scale efficiencies up to 80% can even be expected.

Frequent discussions with the propeller manufacturer during this study allowed the propeller to be specified better and finally a satisfactory one to be obtained. Such cooperation between airplane and propeller manufacturers should doubtlessely be of great benefit for future studies.

	FS	WT
η(HLPQ)/η(deck FS)	1.	0.974

Table 3

3.3. Panel method and Boundary Layer calculations for nacelle design

The FP3D panel method associated with the 3C3D boundary layer code was widely used for the design of the nacelles to be mounted on our FLA model. They allowed quick inviscid analysis of numerous nacelle shapes with a preliminary approach to their viscous behavior, to make sure that no important boundary layer separation would occur.
This paragraph presents some results for two nacelles that could be tested during the first wind-tunnel campaign (nacelles M3 and M7), and some others for an intermediate shape (nacelle M5), that has finally been rejected.
Calculations were performed at cruise conditions (M=0.68, α=3°). Stagnation pressure and temperature needed for 3C3D simulations were taken close to those of S1-Modane.

The main difference between nacelles M3 and M5 (or M7) lies in their length (figures 15 and 16) : the aft part of the short nacelle (M3) intersects the wing inner surface at approximately 55% of the chord, while the long ones (M5 or M7) go further down from the wing trailing edge. M7 nacelles have been generated from M5 nacelles after several iterations. One of the geometric differences between these two nacelles lies in the wing-nacelle intersection which has been optimized for the M7 nacelles. Another one is the lower tail angle of the M7 nacelle, resulting in an expected lower recompression gradient in this region.

The panel method FP3D was first used to roughly apprehend the perfect fluid flow behavior around the geometries : figures 15 and 16 show isolines of the pressure coefficient over the two M3 and M7 geometries.

The main differences in the flow fields are :
- the recompression gradient is higher on the short nacelle rear part than on the long one because of the larger tail angle on the short nacelle,
- for the long nacelles, the critical recompression regions (in terms of boundary layer separation risks) of the nacelles and wing are located in the same area, whereas in the short nacelle case, the wing critical recompression zone occurs downwind of the nacelle one.

Boundary layer calculations were then performed from these FP3D calculations. Figures 17 and 18 show the parietal streamlines on the wing lower surface and outboard nacelle internal parts for both M3 and M7 geometries.

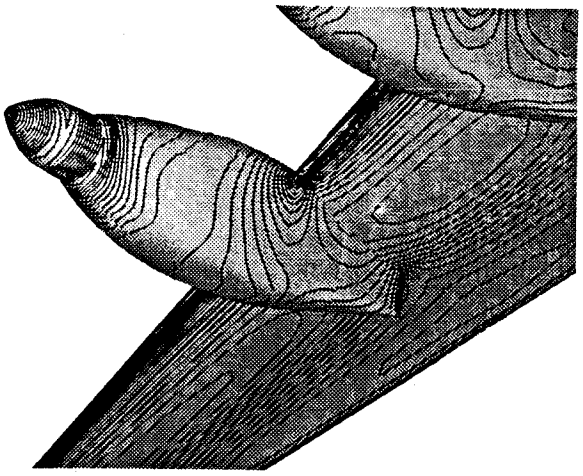

Figure 15
Iso-Cp lines on the outboard M3 nacelle

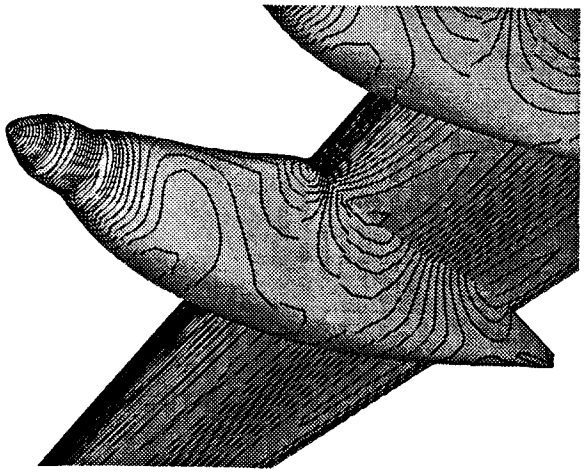

Figure 16
Iso-Cp lines on the outboard M7 nacelle

Apart from small regions on the rear part of the nacelles, the boundary layer shows no sign of separation. Figure 19 shows the same kind of calculations with M5 nacelles. While the parietal streamlines have a quite smooth behavior on the inboard side of the outer M7 nacelle, they dangerously accumulate for the M5 nacelle, leading to a region where the calculation stops (region without streamlines), which is the sign of a probable separation area.

Propeller effects on the viscous behavior of M7 nacelles were then investigated. Figure 20 shows the pressure coefficient distribution on one section of the outer nacelle. The recompression gradients are greater with the propeller on, therefore increasing the boundary layer separation risk. The boundary calculation presented on figure 21 confirms this assertion : the deviation of the parietal streamlines is more pronounced than with the propeller off (compare to figure 18), and streamlines tend to accumulate on the rear part of the nacelles, near the region of maximum recompression of the wing. However, no evident signs of large boundary layer separation regions are present.

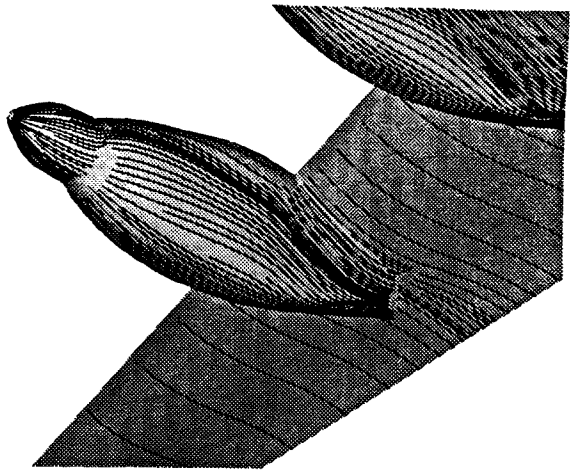

Figure 17
Parietal streamlines on the outboard M3 nacelle

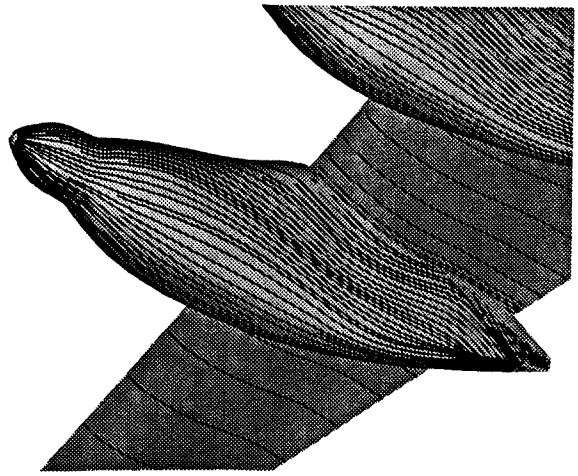

Figure 18
Parietal streamlines on the outboard M7 nacelle

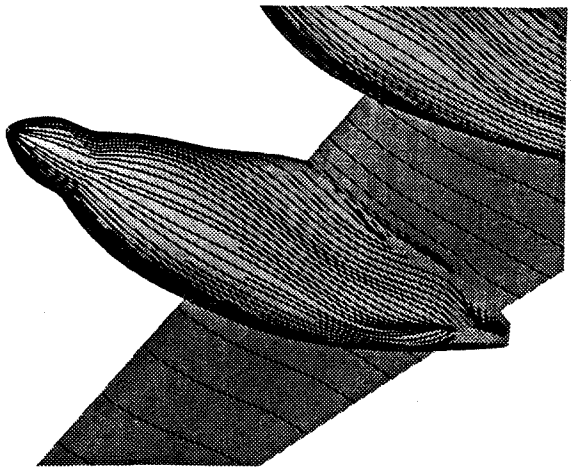

Figure 19
Parietal streamlines on the outboard M5 nacelle

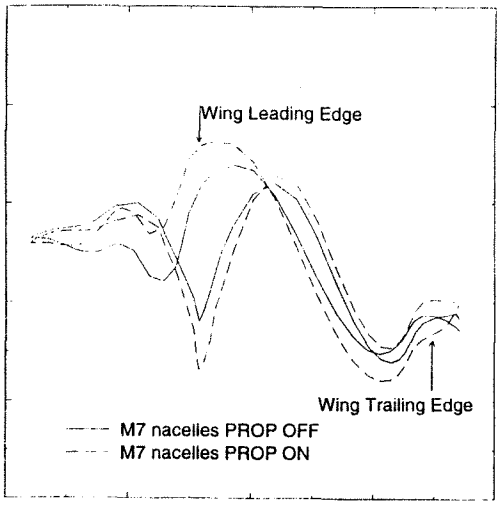

Figure 20
Pressure coefficient distribution on
the outboard M7 nacelle
Effect of propeller blowing

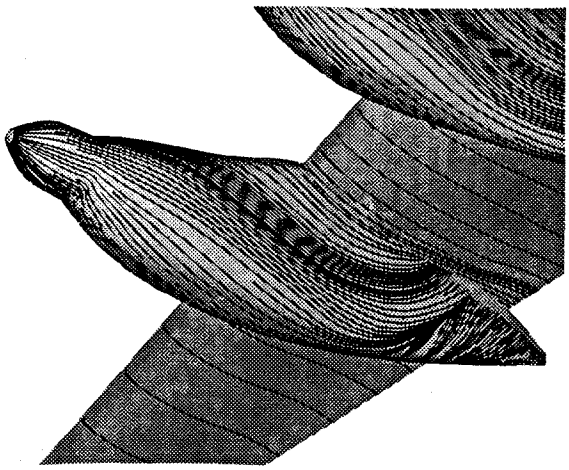

Figure 21
Parietal streamlines on the outer M7 nacelle
propeller on

3.4. Euler calculations about the complete model configuration

Several simulations with both MGAERO and CANARI Euler solvers were performed with the different nacelle geometries on the complete model configuration, in the cruise conditions described in the previous paragraph. Wing fuselage simulations were also made in order to quantify nacelle installation effects. As for FP3D, propeller-off and propeller-on calculations were done leading to a preliminary assessment of the propeller blowing effect, in transonic conditions, before going to the wind-tunnel to get an experimental confirmation.

We first describe the MGAERO and CANARI grids that were constructed for these calculations, before presenting some results on the wing nacelle interaction and propeller blowing effects.

MGAERO grids

Meshes of about 20,000 panels defining the geometry, and volumic meshes of nearly 700,000 grid points were constructed for MGAERO simulations.
The paneling on the wing was refined near the leading edge to get a better geometric precision in this region where high presssure gradients occur (figure 22).
Volumic meshes are composed of 7 embedded levels, level n being roughly twice as fine as level n-1. The first four levels are composed of size decreasing boxes around the complete configuration. The level 5 boxes are presented on figure 22 : one is aligned with the wing leading edge, one with the wing trailing edge, and the last two each recover a nacelle. Figure 23 shows a part of the level 6 and 7 meshes, which are located around the wing leading edge.

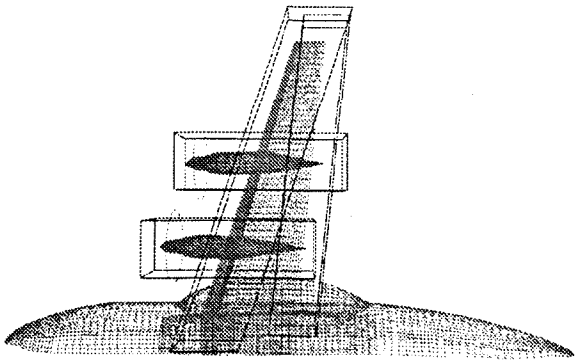

Figure 22
Geometry and level 5 mesh for MGAERO

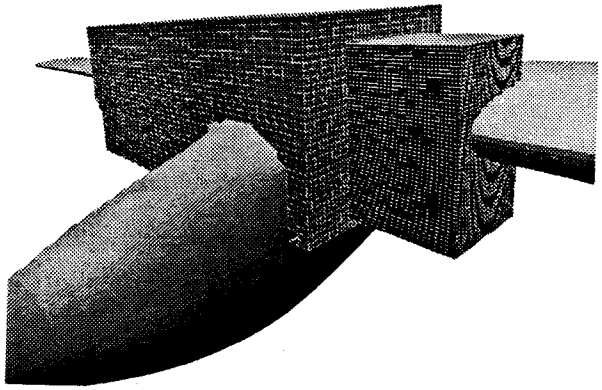

Figure 23
Geometry and level 6-7 mesh for MGAERO

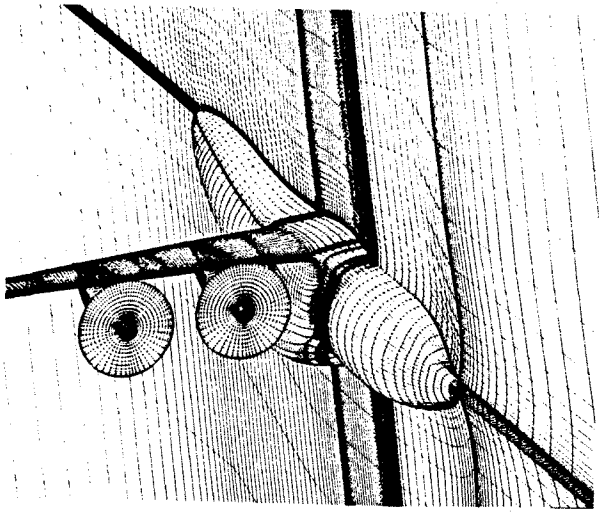

Figure 24
Volumic grid for CANARI simulations
on the complete model configuration

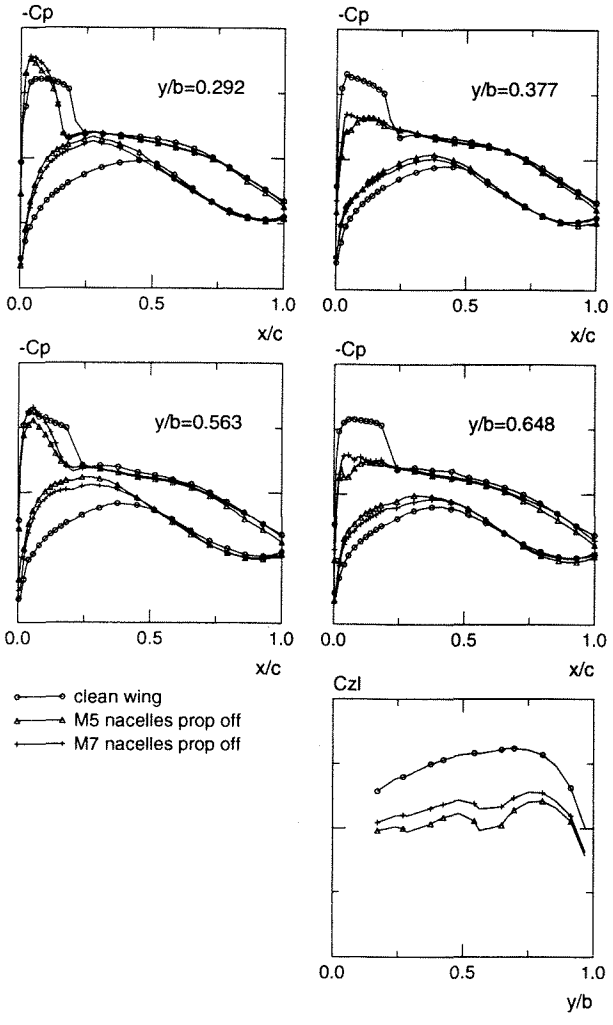

Figure 25
MGAERO - Nacelle installation effect on
wing pressure distributions

CANARI grids

A fine grid about the wing fuselage configuration, and two others about the complete model configuration, with nacelles M5 and M7 respectively, were constructed for CANARI. Composed of 119 domains and nearly 2,000,000 grid points, these last two grids include C-blocks around the wing and O-blocks around the fuselage and nacelles, which allows for a better control of mesh orthogonality near the model surface. Furthermore, it would allow Navier-Stokes grids to be constructed easily, by refining the original Euler grids along the normal direction, which is the technique usually used at Aerospatiale for that purpose. Figure 24 shows the grid with M5 nacelles over the model surface, the propeller disks and the symmetry plane.

Engine installation effect

This section compares the results obtained with MGAERO and CANARI on the clean wing configuration and two engined configurations (M5 and M7 nacelles).

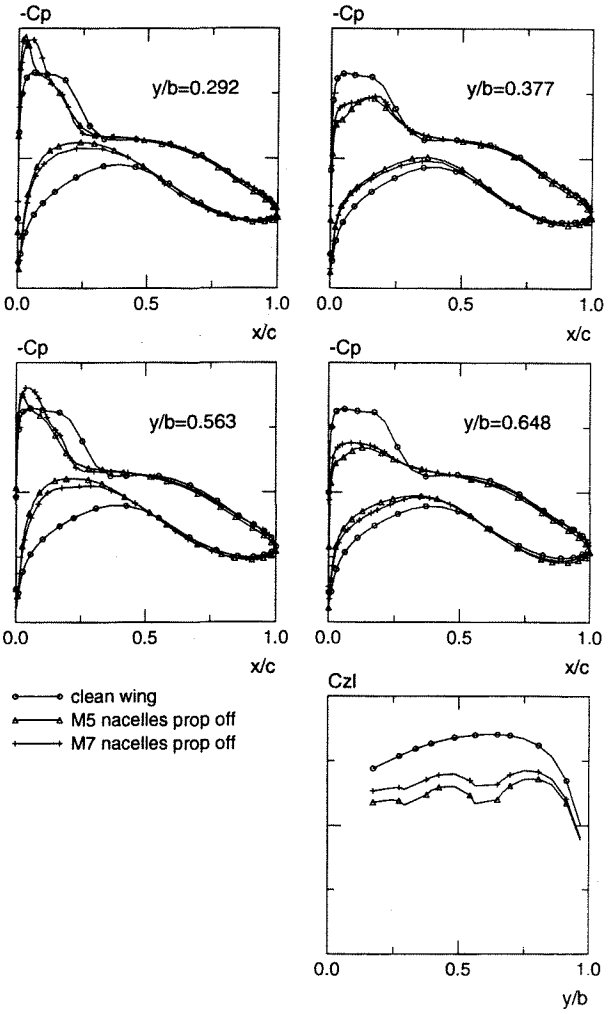

Figure 26
CANARI - Nacelle installation effect on
wing pressure distributions

Pressure distributions are presented on four sections located on each side of both inner and outer nacelles, together with local lift distributions on the wing (figure 25 for MGAERO, figure 26 for CANARI).

Both codes evidence the same effects of the nacelles on the wing pressure field :
- on the inboard side of the nacelles (y/b=0.292 and y/b=0.563), a higher suction peak and a more forward location of the shock on the wing upper surface, and a large acceleration zone (approximately 50% of the chord) on the wing lower surface,
- On the outboard side (y/b=0.377 and y/b=0.648), a very important decrease in the upper surface suction peak, with complete vanishing of the shock, and a slight acceleration of the flow on the wing lower surface.
All these phenomena combine to induce a lift loss, which can be seen on the local lift curves.

The optimization of the nacelle lines for the M7 configuration results in a significative increase (about 8%) in lift coefficient. This increase is mainly due to :
- a rearward displacement of the upper surface shock,
- a global deceleration on the wing lower surface.

Propeller blowing effect

Figure 27 compares the Mach contours given by CANARI on the upper surface of the model equipped with M5 nacelles, with (c) and without (b) propeller blowing. Propeller effects imply a better balance of the suction peak level between the inboard and outboard sides of the two nacelles.
This is confirmed by figures 28 (MGAERO) and 29 (CANARI) which present the same four Cp distributions and local lift distribution as previously shown for nacelle shape effect analysis. The main propeller effect on the wing consists in a modification of local angles-of-attack (axial effects appear to be of second order in cruise conditions). On the inboard sides of the nacelles, the sense of rotation of the propellers induces a local angle-of-attack decrease leading to a decrease in local lift. The contrary effect is evidently observed on the outboard sides of the nacelles. More precisely, the upper surface large suction peak levels induced by nacelle installation on their inboard sides are quite completely erased, whereas on their outboard sides, the suction peak levels are increased, leading to the better balance mentioned before. The levels obtained come back to a value close to those observed on the clean wing. On the wing lower surface, the flow acceleration on the inboard side of the nacelles is more pronounced than the outboard deceleration.
Once again the agreement between the two solvers is quite satisfactory : effects are well reproduced by MGAERO, which tends nevertheless to underestimate absolute levels.
Experimental data will make it possible to complete the calibration of both codes and thus to use them, in the next steps of the FLA design process, in an even more efficient way. Complementary to these wind-tunnel results on the left wing, calculations will then help in designing an optimized engine installation that would account for both wings.

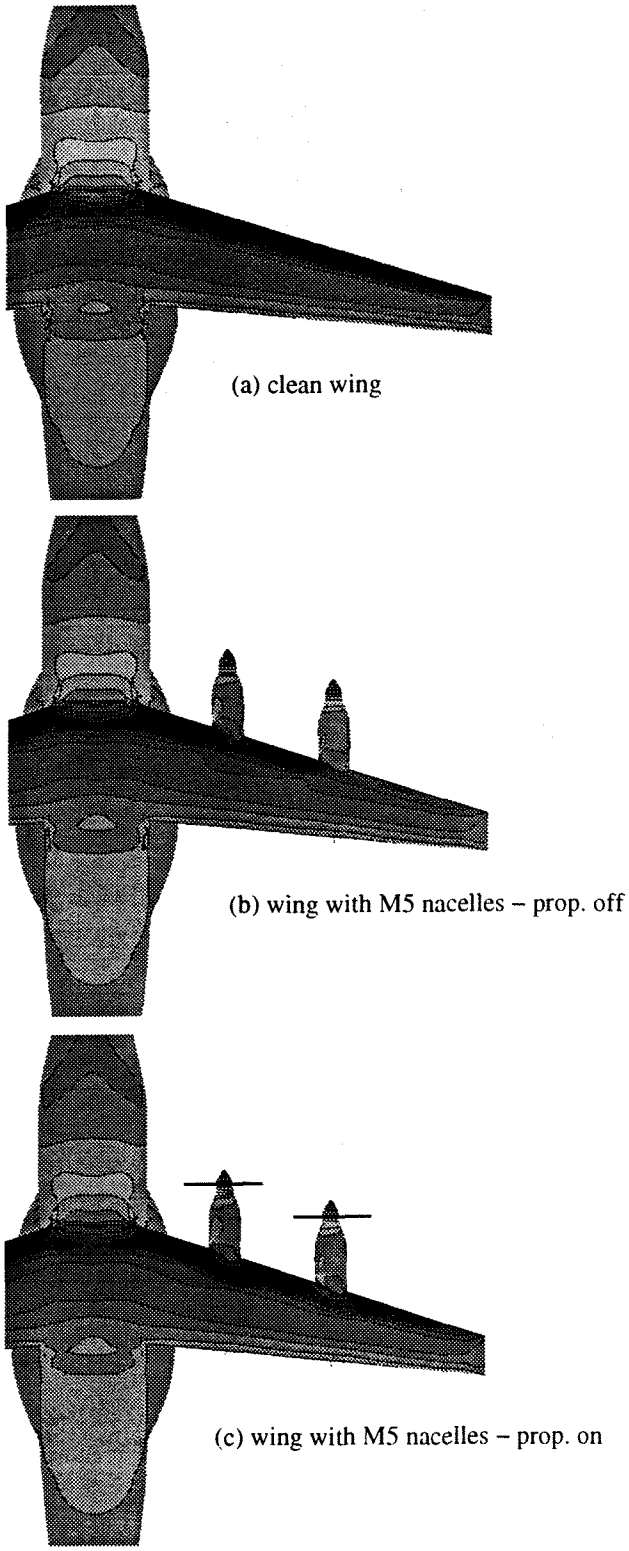

Figure 27
CANARI calculations
Mach contours on the clean wing (a) and on the wing with M5 nacelles with (b) and without (c) propeller blowing

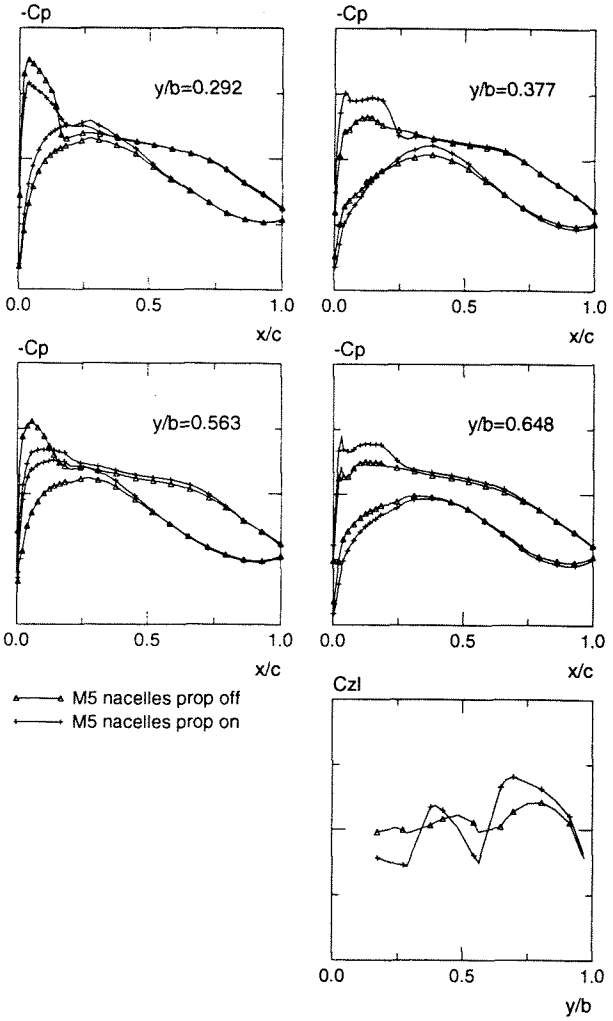

Figure 28
MGAERO - Propeller effect on
wing pressure distributions

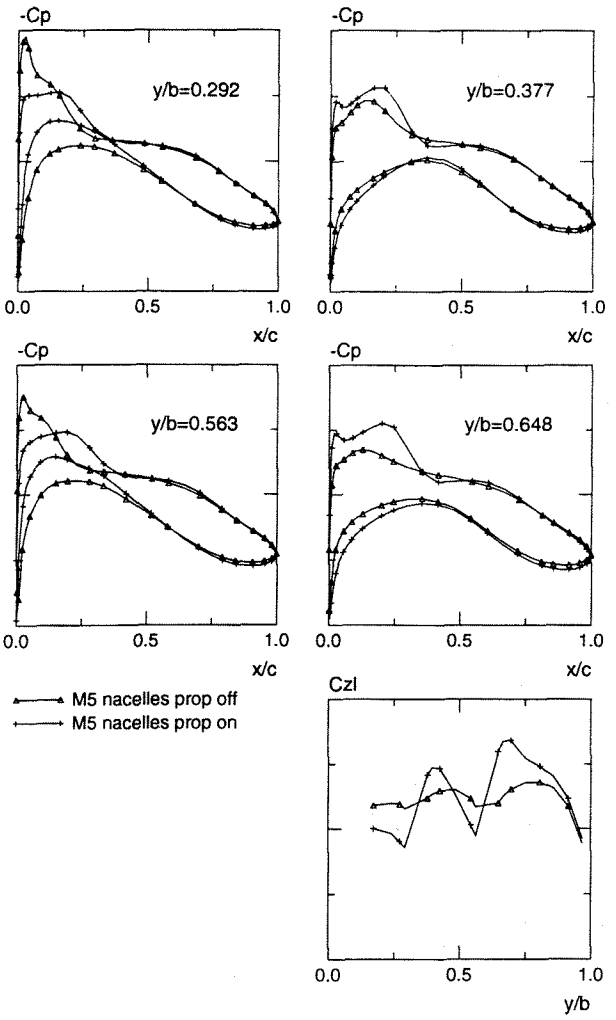

Figure 29
CANARI - Propeller effect on
wing pressure distributions

4. Conclusion

Aerospatiale has quite a complete numerical toolkit available for aerodynamic analysis of propeller driven aircraft configurations : from a simple panel method for preliminary investigations to Euler solvers for more realistic transonic calculations, all of them allowing for propeller blowing modelling.

Together with isolated propeller simulations codes, these solvers provide the design engineer with analysis means which are well suited for the different steps of the aerodynamic design process of a new aircraft, and particularly, as far as Aerospatiale is concerned, for engine integration studies.

These tools have been used within the framework of the design of a FLA model for various tasks :
- choice of the propeller to be mounted on the model,
- definition of nacelle external shapes,
- first assessment of propeller wake / airframe interaction.

Completion of first wind-tunnel tests with this model will provide a large amount of information which will be used to continue the validation of these different solvers. They will then be well calibrated and ready to be intensively used for the next phases of the FLA engine installation design.

References

(1) D.Bertin, J.Lordon, V.Moreux : "A New Automatic Grid Generation Environment for CFD Applications", AIAA-92-2720-CP, 10th AIAA Applied Aerodynamics Conference, 1992

(2) R.Collercandy : "Etude et calcul théorique d'écoulements transsoniques autour d'une hélice propulsive de type propfan", thesis, Pierre et Marie Curie (Paris VI) University, July 1984

(3) R.Siestrunck : "Le développement moderne de la théorie de l'hélice", Institut de Mécanique de la Faculté des Sciences de Paris, 1947

(4) M.Drela, M.B.Giles : "ISES : A Two-Dimensionnal Viscous Aerodynamic Design and Analysis Code", AIAA Paper 87-0424, 1987

(5) C.Kirrmann, A.Rousseau, M.Yermia : "Calcul du souffle moyen d'une hélice et de son influence sur les performances d'un avion", l'Aéronautique et l'Astronautique, n° 104-1984-1, 1984

(6) X.Monthus, P.Colin, P.Mogilka, A.Molbay-Arsan : "Utilisation des méthodes de calcul pour optimiser l'installation motrice des avions de transport", AGARD Symposium on Recent Advances in Long Range and Long Endurance Operation of Aircraft, The Hague, May 24-27, 1993

(7) P.Colin, P.Mogilka, A.Molbay-Arsan : "CFD Analysis of Engine / Airframe Interference for Advanced Integration Studies on Transport Aircraft", RAeS European Forum, Bristol , September 1-3, 1993

(8) P.Mogilka, P.Colin, N.Esteve : "Aerodynamic Study of New Engine / Airframe Integration Concepts", 19th ICAS Congress, Anaheim, September 18-23, 1994

(9) A.M.Vuillot, V.Couaillier, N.Liamis : "3D Turbomachinery Euler and Navier Stokes Calculations with a Multi-domain Cell Centered Approach", 29th AIAA/SAE/ASME/ASEE Joint Propulsion Conference, AIAA 93-2576, Monterey, June 28-July 1, 1993

(10) V.Couaillier : "Recent Developments Performed at Onera for the Simulation of 3D Inviscid and Viscous Flows in Turbomachinery by the Solution of Euler and Navier-Stokes Equations", 11th ISABE Conference, Tokyo, September 20-24, 1993

(11) A.Jameson, W.Schmidt, E.Turkel : "Numerical Solution of the Euler Equations by Finite Volume Methods Using Runge-Kutta Time Stepping Schemes", AIAA Paper 81-1259, 1981

(12) J.Bousquet, P.Eichel, V.Rivoire, T.Surply : "Integral methods, theoretical and practical aspects", CLARENDON PRESS-OXFORD, edited by P.STOW, 1990

(13) B.Hunt : "Recent and anticipated advances in the panel method : the key to generalized field calculations", VKI lecture (CFD), March 1980

(14). D.J. Strash : "MGAERO User's Manual, Version 3.0", Analytical Methods, Inc., Redmond WA, 1996

(15). D.M. Tidd, D.J. Strash, B. Epstein, A. Luntz, A., Nachshon, T. Rubin : "Multigrid Euler Calculations over Complete Aircraft", Journal of Aircraft, Vol. 29, No. 6, Nov-Dec. 1992

(16). R. Houdeville, P. Malecki : "Calculs de Couches Limites Tridimensionnelles. Description et Mode d'Emploi du code 3C3D. Version 5.2.2.1", DERAT Technical Report No. 63/5625.54, September 1995

(17). R. Houdeville : "Three-Dimensional Boundary Layer Calculation by a Characteristic Method", fifth Symposium on Numerical and Physical Aspects of Aerodynamic Flows, Long Beach, January 1992